

# LOW TEMPERATURE SUPERFLUID RESPONSE OF HIGH- $T_c$ SUPERCONDUCTORS

T. XIANG<sup>1,2</sup>, C. PANAGOPOULOS<sup>1</sup>, AND J. R. COOPER<sup>1</sup>

<sup>1</sup>*Interdisciplinary Research Center in Superconductivity, University of Cambridge,  
Madingley Road, Cambridge CB3 0HE, United Kingdom*

<sup>2</sup>*Institute of Theoretical Physics, Academia Sinica, P.O.Box 2735, Beijing 100080, China*

## Abstract

We have reviewed our theoretical and experimental results of the low temperature superfluid response function  $\rho_s^\mu$  of high temperature superconductors (HTSC). In clean high- $T_c$  materials the in-plane superfluid density  $\rho_s^{ab}$  varies linearly with temperature. The slope of this linear  $T$  term is found to scale approximately with  $1/T_c$  which, according to the weak coupling BCS theory for a  $d$ -wave superconductor, implies that the gap amplitude scales approximately with  $T_c$ . A  $T^5$  behavior of the out-of-plane superfluid density  $\rho_s^c$  for clean tetragonal HTSC was predicted and observed experimentally in the single layer Hg-compound  $\text{HgBa}_2\text{CuO}_{4+\delta}$ . In other tetragonal high- $T_c$  compounds with relatively high anisotropy, such as  $\text{Hg}_2\text{Ba}_2\text{Ca}_2\text{Cu}_3\text{O}_{8+\delta}$ ,  $\rho_s^c$  varies as  $T^2$  due to disorder effects. In optimally doped  $\text{YBa}_2\text{Cu}_3\text{O}_{7-\delta}$ ,  $\rho_s^c$  varies linearly with temperature at low temperatures, but in underdoped  $\text{YBa}_2\text{Cu}_3\text{O}_{7-\delta}$ ,  $\rho_s^c$  varies as  $T^2$  at low temperatures; these results are consistent with our theoretical calculations.

## 1 Introduction

A growing number of theoretical and experimental works have showed that the high- $T_c$  superconducting pairing has  $d_{x^2-y^2}$  symmetry<sup>1</sup>. The existence of energy gap nodes in this state has profound consequences for the low temperature electromagnetic response. In high quality single crystal or magnetically aligned powder high- $T_c$  superconductors (HTSC), it has been found that the in-plane penetration depth  $\lambda_{ab}$ , whose temperature ( $T$ ) dependence is determined by the thermal excitations of unpaired electrons, increases linearly with  $T$  at low  $T$ , in contrast to the activated behavior of conventional superconductors. The intrinsic linear- $T$  behavior of  $\lambda_{ab}$  was first observed in a twinned  $\text{YBa}_2\text{Cu}_3\text{O}_{7-\delta}$  single crystal<sup>2</sup> and was one of the earliest pieces of evidence for the  $d$ -wave symmetry of the gap parameter. The linear- $T$  behavior of  $\lambda_{ab}$  has now been established in both chain and nonchain copper oxides, which include optimally doped or underdoped  $\text{YBa}_2\text{Cu}_3\text{O}_{7-\delta}$ <sup>2,3,4,5,6</sup>,  $\text{Bi}_2\text{Sr}_2\text{CaCu}_2\text{O}_{8+\delta}$ <sup>7,8</sup>,  $\text{HgBa}_2\text{CuO}_{4+\delta}$ <sup>9</sup>,  $\text{HgBa}_2\text{Ca}_2\text{Cu}_3\text{O}_{8+\delta}$ <sup>9,10</sup>,  $\text{Tl}_2\text{Ba}_2\text{CuO}_{6+\delta}$ <sup>11</sup>, and  $\text{La}_{2-x}\text{Sr}_x\text{CuO}_4$ <sup>12</sup>.

The temperature dependence of the  $c$ -axis penetration depth has also been measured in a variety of high- $T_c$  compounds, such as  $\text{YBa}_2\text{Cu}_3\text{O}_{7-\delta}$ <sup>4,5,9</sup>,  $\text{La}_{2-x}\text{Sr}_x\text{CuO}_4$ <sup>13</sup>,  $\text{Bi}_2\text{Sr}_2\text{CaCu}_2\text{O}_{8+\delta}$ <sup>7</sup>,  $\text{HgBa}_2\text{CuO}_{4+\delta}$  and  $\text{HgBa}_2\text{Ca}_2\text{Cu}_3\text{O}_{8+\delta}$ <sup>9</sup>. A common feature revealed in all measurements is that the  $T$  dependence of the  $c$ -axis penetration depth is much weaker than its in-plane counterpart at low  $T$ . It has been found that  $\lambda_c(T)$  approaches to its zero temperature value as a power law, namely

$\lambda_c(T) - \lambda_c(0) \sim T^n$ , with  $n$  often being sample dependent and generally greater than 1.

Understanding why the temperature dependence of  $\lambda_c$  in high- $T_c$  superconductors is much weaker than  $\lambda_{ab}$  is not a trivial problem. Straightforward extension of the 2D  $d$ -wave model to anisotropic 3D leads to line nodes on a warped cylindrical Fermi surface. This gives a strong linear- $T$   $c$ -axis response in apparent contradiction to experiment.

The weak  $T$  dependence of  $\lambda_c$  is actually an intrinsic feature of HTSC. As shown by Xiang and Wheatley<sup>14,15</sup>, it is due to the interplay between the  $d$ -wave symmetry of the superconducting order parameter and the underlying Cu 3*d*-orbital-based electronic structure of copper oxides. For high- $T_c$  compounds with tetragonal symmetry, they predicted<sup>15</sup> that in the clean limit  $\lambda_c$  should behave as  $T^5$  at low  $T$ . Recently this  $T^5$  behavior was observed experimentally in the single layer Hg-compound by Panagopoulos et al<sup>9</sup>. As in the case of  $\lambda_{ab}$ , impurity scattering can have a strong impact on the  $T$  dependence of  $\lambda_c$ <sup>15,16,17</sup>. In the temperature regime where impurity scattering is important,  $\lambda_c$  generally behaves as  $T^2$  or  $T^3$ , depending on the type and strength of the scattering potentials<sup>15,16,17</sup>.

It is possible that the normal state of HTSC is a non-Fermi liquid. However, in the superconducting state, the behavior of high- $T_c$  materials does not deviate significantly from that of conventional metallic superconductors except the different pairing symmetry. Moreover, angle-resolved photoemission spectroscopy (ARPES) experiments<sup>18</sup> show that BCS quasiparticle excitations exist at  $T \ll T_c$ . Thus it is generally agreed that the BCS theory is applicable to HTSC at least at low  $T$ .

To understand the interlayer dynamics in the superconducting phase, a key issue which needs to be clarified is whether the interlayer hopping of superconducting quasiparticles is coherent or incoherent. In normal states the  $c$ -axis mean free path is short compared with the  $c$ -axis lattice constant. The semiconducting behavior of the out-of-plane normal state resistivity  $\rho_c$  has generally been taken as evidence that the  $c$ -axis transport cannot be described by conventional three dimensional coherent Bloch transport. Microwave<sup>19</sup> and thermal Hall measurements<sup>20</sup>, however, revealed that the mean free path increases by more than six orders of magnitude in the superconducting state. The superconducting quasiparticle scattering rate is therefore much lower than the extrapolated normal state scattering rate. Thus it is our belief that excited quasiparticles form coherent Bloch band along the  $c$  axis in the superconducting state at low  $T$ . For  $\text{Bi}_2\text{Sr}_2\text{CaCu}_2\text{O}_{8+\delta}$  or other extremely anisotropic compounds, the coherent tunneling is small and the  $c$ -axis superfluid response might still be dominated by the impurity assisted hopping<sup>16</sup>. However, for other compounds with tetragonal crystal symmetry and lower anisotropy, we believe that the coherent band should give a substantial contribution to the  $c$ -axis superfluid response function.

This paper arranges as follows. In Sec. 2 a general formula for the superfluid response function is derived from standard linear response theory. In Sec. 3, we analyse the electronic structures of copper oxides and the low  $T$  behaviors of the superfluid response tensor, concentrating particularly on the properties of  $\lambda_c$ . Sec. 4 discusses the effects of disorder on  $\lambda_c$ . In Sec. 5, we present experimental results for both  $\lambda_{ab}$  and  $\lambda_c$  in a variety of high- $T_c$  materials. A brief introduction to the

technique we used in obtaining the experimental data is also given in this section. Finally, Sec. 6 summarizes the results.

## 2 Superfluid response function

According to the London equation, the superfluid density is inversely proportional to the square of the penetration depth. From linear response theory<sup>21</sup>, it can be shown that the superfluid tensor is given by

$$\rho_s^\mu = K_\mu + \Lambda_\mu \quad (1)$$

$$K_\mu = \frac{1}{\Omega} \sum_{k\sigma} \frac{\partial^2 \varepsilon_k}{\partial k_\mu^2} \langle c_{k\sigma}^\dagger c_{k\sigma} \rangle, \quad (2)$$

$$\Lambda_\mu = -\frac{1}{\Omega} \lim_{k \rightarrow 0} \int_0^\beta d\tau \langle J_\mu(k, \tau) J_\mu(-k, 0) \rangle, \quad (3)$$

where  $\langle \rangle$  denotes a thermal average,  $\varepsilon_k$  is the band energy of electrons, and  $J_\mu(k) = \sum_{q\sigma} (\partial \varepsilon_q / \partial q_\mu) c_{q\sigma}^\dagger c_{q-k\sigma}$  is the current operator.  $\Omega$  is the volume of the system.  $K_\mu$  and  $\Lambda_\mu$  are the diamagnetic and paramagnetic responses of quasiparticles to an external field, respectively. Generally  $K_\mu$  is weakly temperature dependent but  $\Lambda_\mu$  is strongly temperature dependent. For a spherical energy band,  $\varepsilon_k = k^2/2m^* - \mu$ ,  $K_\mu = n/m^*$  is temperature independent, where  $n$  is the electron concentration. Above  $T_c$ , the contribution from  $\Lambda_\mu$  cancels that from  $K_\mu$ , leading to a zero superfluid density. Below  $T_c$ ,  $\Lambda_\mu$  decreases with decreasing temperature.

In the weak coupling BCS theory, Eqs. (2) and (3) can be simplified to

$$K_\mu = \frac{1}{\Omega} \sum_k \frac{\partial^2 \varepsilon_k}{\partial k_\mu^2} \left( 1 - \frac{\varepsilon_k}{E_k} \tanh \frac{\beta E_k}{2} \right), \quad (4)$$

$$\Lambda_\mu = \frac{1}{\Omega} \sum_k 2 \left( \frac{\partial \varepsilon_k}{\partial k_\mu} \right)^2 \frac{\partial f(E_k)}{\partial E_k}, \quad (5)$$

for a single band system. Here  $E_k = \sqrt{\varepsilon_k^2 + \Delta_k^2}$  and  $\Delta_k$  is the gap order parameter. For an anisotropic  $d$ -wave superconductor with  $\varepsilon_k = (1/2m_a^*)(k_x^2 + k_y^2) - 2t_\perp \cos k_z - \mu$ ,  $\Delta_k = \Delta_0 \cos(2\phi)$ ,  $\phi = \arctan(k_y/k_x)$ , and  $m_a^* \ll t_\perp^{-1}$ , it is straightforward to show that

$$\rho_s^{a,b} \approx \frac{n}{m_a^*} \left( 1 - \frac{(2 \ln 2)T}{\Delta_0} \right), \quad (6)$$

$$\rho_s^c \approx \frac{2m_a^* t_\perp^2}{\pi} \left( 1 - \frac{(2 \ln 2)T}{\Delta_0} \right), \quad (7)$$

up to the leading order approximation of  $T$  and  $t_\perp$ .  $\rho_s^c$  is different than  $\rho_s^{a,b}$  because of the anisotropy, but the normalized superfluid density  $\rho_s^\mu(T)/\rho_s^\mu(0)$  is approximately the same in all three directions. The linear  $T$  dependence of  $\rho_s^\mu$  is a direct consequence of the linear low energy density of states of a  $d$ -wave superconductor.

The linear  $T$  dependence of  $\rho_s^{a,b}$  in this anisotropic system is consistent with experimental results of HTSC. However, the  $T$  dependence of  $\rho_s^c$  given by Eq. (7) is too strong compared with experiments, which indicates that this simple model of an anisotropic  $d$ -wave superconductor is insufficient to account for the experimental data.

### 3 Low $T$ behaviors of superfluid tensor

In this section, we discuss the properties of the electronic structure of HTSC and analyse why  $\rho_s^c$  has a weaker  $T$  dependence than  $\rho_s^{a,b}$ . We consider first the tetragonal (or almost tetragonal) HTSC, and then  $\text{YBa}_2\text{Cu}_3\text{O}_{7-\delta}$  materials. In  $\text{YBa}_2\text{Cu}_4\text{O}_8$ , where two neighboring CuO chain layers are offset by  $b/2$ , the coupling between two neighboring CuO chain layers is therefore very different from that between a CuO layer and a  $\text{CuO}_2$  layer. To understand the properties of  $\rho_s^\mu$  of  $\text{YBa}_2\text{Cu}_4\text{O}_8$ , a proximity  $(NSSN)(NSSN)'$  model should be considered, where  $S$  represents a  $\text{CuO}_2$  layer,  $N$  a CuO layer, and  $(NSSN)'$  represents a unit cell which is offset by  $b/2$  along the  $b$ -axis with respect to its neighboring unit cell  $(NSSN)$ . At present a detailed study for this complicated  $(NSSN)(NSSN)'$  model has not been made.

#### 3.1 Tetragonal compounds

The electronic structure of high- $T_c$  oxides is mainly determined by the O  $2p_x, 2p_y$  and Cu  $3d_{x^2-y^2}, 4s$  orbitals (Fig. 1). The wavefunctions of the first three orbitals extend mainly along the short Cu-O bond axes, leading to a large Cu-O hopping integral in the  $ab$  plane. The O  $2p$  can be classified as bonding and non-bonding Wannier orbitals according to their interaction with Cu  $3d$  orbitals. The non-bonding O  $2p$  orbital, which has a zero wavefunction overlap with Cu  $3d$ , is believed to be filled and has little effect on the low  $T$  transport properties of cuprates. Thus only the bonding O orbitals need be considered. In the limit of strong Coulomb repulsion, each doped hole on the bonding O  $2p$  orbital will form a local Zhang-Rice spin singlet with a Cu spin<sup>22</sup>. The low energy physics of high- $T_c$  oxides is governed by this singlet band. The Cu  $4s$  has a much higher energy than the Fermi level. However, it is important for the interlayer hopping of holes<sup>23</sup>, since the interlayer hopping is mainly assisted by the Cu  $4s$  orbitals. It also has a large contribution to the 2nd and 3rd nearest neighbor ( $t'$  and  $t''$ ) intra-plane hopping integrals.

The interlayer hopping of holes is accomplished through the following virtual hopping processes<sup>15,24</sup>: a hole first hops from an O  $2p$  to a Cu  $4s$  orbital on one  $\text{CuO}_2$  plane, then hops to another Cu  $4s$  on an adjacent  $\text{CuO}_2$  plane via some intermediate orbitals between these two planes, and finally hops to an O  $2p$  orbital on the second plane. Schematically, this interlayer hopping process can be represented as

$$(\text{O } 2p)_1 \rightarrow (\text{Cu } 4s)_1 \rightarrow (*)_{12} \rightarrow (\text{Cu } 4s)_2 \rightarrow (\text{O } 2p)_2,$$

where the subscripts '1' and '2' denote the first and second CuO layer, respectively.  $(*)_{12}$  represents all relevant orbitals between two CuO layers. A doped hole has a certain probability to occupy the Cu  $3d_{x^2-y^2}$  orbitals. However, as Cu  $3d_{x^2-y^2}$  and

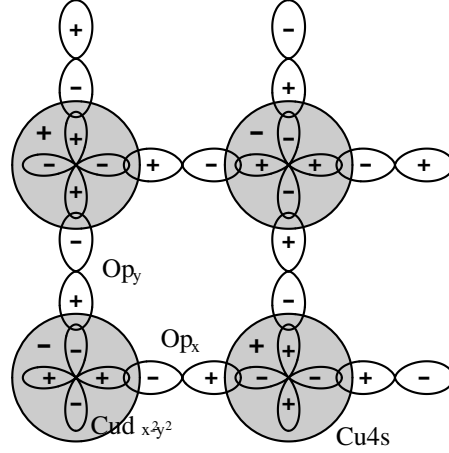


Figure 1: Cu  $3d_{x^2-y^2}$  and  $4s$  and O  $2p_x$  and  $2p_y$  orbitals on each CuO plane.

$4s$  orbitals are orthogonal to each other, a Cu  $3d$  hole cannot hop directly to a Cu  $4s$  orbital.

The hopping integral from  $(O\ 2p)_1$  to  $(O\ 2p)_2$  is proportional to the product of each individual virtual hopping process, hence the interlayer hopping integral,

$$\varepsilon_{\perp} \propto \langle (2p)_2 | (4s)_2 \rangle \langle (4s)_2 | (*)_{12} \rangle \langle (*)_{12} | (4s)_1 \rangle \langle (4s)_1 | (2p)_1 \rangle.$$

The wavefunction overlap between Cu  $4s$  and  $(*)_{1-2}$  is generally expected to be weakly dependent on  $k_{\parallel} = (k_x, k_y)$ . However, the wavefunction overlap between the bonding O  $2p$  and Cu  $4s$  state has  $d_{x^2-y^2}$  symmetry (Fig 1), i.e.  $\langle (4s) | (2p) \rangle$  is proportional to  $\cos k_x - \cos k_y$ , in each tetragonal  $\text{CuO}_2$  plane. Thus  $\varepsilon_{\perp} \propto (\cos k_x - \cos k_y)^2$ , which vanishes along two diagonal directions of the in-plane Brillouin zone. This is a unique property of high- $T_c$  oxides.

The relation  $\varepsilon_{\perp}(k_{\parallel}) \propto (\cos k_x - \cos k_y)^2$  implies that there is no splitting in the band energy of electrons along the  $(0,0) - (\pi, \pi)$  direction for different  $k_z$  cross sections. This property was actually first found in LDA band structure calculations<sup>23</sup> and is supported by all LDA calculations of high- $T_c$  cuprates with tetragonal symmetry<sup>25</sup>.

The above discussion indicates that the factor  $(\cos k_x - \cos k_y)^2$  in  $\varepsilon_{\perp}$  comes from the *in-plane* wave function overlap in two  $\text{CuO}_2$  planes. Thus  $\varepsilon_{\perp} \propto (\cos k_x - \cos k_y)^2$  holds for all high- $T_c$  cuprates with tetragonal symmetry, independently of the number of  $\text{CuO}_2$  layers per unit cell and the way they are coupled together. In  $\text{La}_{2-x}\text{Sr}_x\text{CuO}_4$  or other body centred tetragonal systems, Cu atoms do not lie collinearly along the  $c$ -axis. This will make the  $k_{\parallel}$  dependence of  $t_{\perp}(k_{\parallel})$  in  $\varepsilon_{\perp}(k_{\parallel}) = t_{\perp}(k_{\parallel})(\cos k_x - \cos k_y)^2$  more complicated, but will not alter the property  $\varepsilon_{\perp} \propto (\cos k_x - \cos k_y)^2$ .

There is a small orthorhombic distortion in  $\text{Bi}_2\text{Sr}_2\text{CaCu}_2\text{O}_{8+\delta}$ ,  $\text{La}_{2-x}\text{Sr}_x\text{CuO}_4$ , and a few other high- $T_c$  compounds. However, as the orthorhombic distortion is along the diagonal direction of the square Cu lattice on CuO planes in these ma-

terials,  $\varepsilon_{\perp} \propto (\cos k_x - \cos k_y)^2$  is still valid even though the  $x$  and  $y$  axes are not exactly perpendicular to each other.

In high- $T_c$  oxides, Cu 4s are always mixed with Cu  $3d_{z^2}$  orbitals. Thus in the above discussion a Cu 4s state should be taken as a mixed state of Cu 4s and  $3d_{z^2}$  orbitals. This mixing, however, does not alter the above discussion because the Cu  $3d_{z^2}$  orbital, like Cu 4s, has rotational symmetry about the  $c$ -axis as well as reflection symmetry in the CuO plane. The overlap between the bonding O  $2p$  and Cu  $3d_{z^2}$  orbitals is also proportional to  $(\cos k_x - \cos k_y)$ .

Knowing that  $\varepsilon_{\perp}(k) = t_{\perp}(k_{\parallel})(\cos k_x - \cos k_y)^2$ , we can now analyse the temperature dependence of  $\rho_s^c$ . Since at low  $T$ , the physical properties of a  $d_{x^2-y^2}$ -wave superconductor are determined by the quasiparticle excitations near the nodes, we can assume  $t_{\perp}(k_{\parallel}) = t_{\perp}$  to be a  $k_{\parallel}$ -independent constant. The zero of  $\varepsilon_{\perp}(k)$  is located along the same direction as the  $d_{x^2-y^2}$  gap nodes. This means that the paramagnetic current is greatly suppressed along the  $c$ -axis at low  $T$ . Thus the  $c$ -axis superfluid density must behave very differently than in an ordinary anisotropic system where  $\rho_s^c$  varies linearly with  $T$  [Eq. (7)]. Indeed, as shown by Xiang and Wheatley<sup>14</sup> and later confirmed experimentally by the Cambridge group<sup>9</sup>,  $\rho_s^c$  varies approximately as  $T^5$  at low  $T$

$$\rho_s^c(T) \approx \frac{3}{4}N(\varepsilon_F)t_{\perp}^2 \left[ 1 - 450 \left( \frac{T}{\Delta_0} \right)^5 \right], \quad (8)$$

where  $\Delta_0$  is the gap maximum at  $T = 0$  and  $N(\varepsilon_F)$  is the normal density of states on CuO<sub>2</sub> planes. This  $T^5$  term is from the contribution of the paramagnetic term: one power of  $T$  is from the linear density of states of the  $d$ -wave superconductor,  $\rho(E) \sim E$ ; the other  $T^4$  is from the  $(\cos k_x - \cos k_y)^4$  factor in  $(\partial \varepsilon_k / \partial k_z)^2 \propto \varepsilon_{\perp}^2(k_{\parallel})$  which is approximately proportional to  $E^4$  at low energy. This  $T^5$  power law of  $\rho_s^c$  is true only if the high- $T_c$  pairing has the  $d_{x^2-y^2}$  symmetry. If the gap nodes are not located along the zone diagonal, such as in a  $d_{xy}$ -wave superconductor, the low temperature behavior of  $\rho_s^c$  will be completely different. Therefore, from the measurement of  $\rho_s^c$  we can determine unambiguously whether the high- $T_c$  pairing has the  $d_{x^2-y^2}$  symmetry.

There are several effects which may lead to a finite hopping integral along the  $c$ -axis in the vicinity of the gap nodes in clean systems and thus a stronger  $T$  dependence of  $\rho_s^c$ . Direct interplane hoppings which are not assisted by Cu 4s orbitals, for example, can make the  $c$ -axis dispersion finite around the gap nodes and eliminate the zeros in  $\varepsilon_{\perp}(k_{\parallel})$  altogether. In this case, we may model the  $c$ -axis electronic structure by  $\varepsilon_{\perp}(k_{\parallel}) = t_{\perp}(\cos k_x - \cos k_y)^2 + t_{\perp}^{\text{node}}$ , where  $t_{\perp}^{\text{node}}$  denotes the interlayer hopping integral at the gap nodes contributed from all possible interlayer hopping channels not assisted by Cu 4s states.  $t_{\perp}^{\text{node}}$  is expected to be small in high- $T_c$  compounds, but it generates a small linear term in  $\rho_s^c$ , with a slope proportional to  $(t_{\perp}^{\text{node}})^2$ , which dominates the  $c$ -axis superfluid response when  $T \ll t_{\perp}^{\text{node}}$ .

### 3.2 YBa<sub>2</sub>Cu<sub>3</sub>O<sub>7- $\delta$</sub> materials

YBCO contains CuO chains. This is the main feature which distinguishes YBCO from other high- $T_c$  compounds. Recently Hardy and co-workers at UBC mea-

sured the penetration depth of untwinned single crystals of  $YBa_2Cu_3O_{7-\delta}$  and  $YBa_2Cu_4O_8$  along the three principal axes<sup>3,4,26</sup>. They found that the ratio of the superfluid density in  $b$  and  $a$  directions at zero temperature is  $\approx 2.4$  for the one-chain compound  $YBa_2Cu_3O_{6.95}$ <sup>26,27</sup> and  $\approx 6$  for the two-chain compound  $YBa_2Cu_4O_8$ <sup>26</sup>. Anisotropies of similar magnitudes are observed in the normal state resistivity as well<sup>28</sup>. This indicates that more than half of the  $b$ -axis superfluid density comes from the contribution of CuO chains. Knight shift and NMR relaxation rate measurements<sup>29,30</sup> in  $YBa_2Cu_3O_{6.95}$  have also revealed that there is an appreciable gap on the chains below  $T_c$ . Thus to understand the properties of the  $c$ -axis electromagnetic response functions in YBCO, we need consider not only the properties of electrons on the CuO<sub>2</sub> planes, but also those on the CuO chains.

An interesting feature revealed by the penetration depth measurement of the one-chain compound  $YBa_2Cu_3O_{7-\delta}$  is that the temperature dependences of the superfluid densities in  $a$  and  $b$  directions are similar: both are linear at low temperature<sup>3,4</sup>, and roughly obey  $\rho_a^{(s)}(T)/\rho_a^{(s)}(0) \simeq \rho_b^{(s)}(T)/\rho_b^{(s)}(0)$  up to  $T_c$ . The linear  $T$  dependence of  $\rho_c^{a,b}$  can be understood from the standard theory of  $d$ -wave superconductors. However, the relation  $\rho_a^{(s)}(T)/\rho_a^{(s)}(0) \simeq \rho_b^{(s)}(T)/\rho_b^{(s)}(0)$  is unexpected. This unexpected result indicates that the CuO chain layers must be intrinsically superconducting, yet there must be a node of the energy gap on the chain Fermi surface sheet. Otherwise, one should observe  $(d\rho_b^{(s)}/dT)|_{T=0} \simeq (d\rho_a^{(s)}/dT)|_{T=0}$ , instead of  $d[\rho_a^{(s)}(T)/\rho_a^{(s)}(0)]/dT|_{T=0} \simeq d[\rho_b^{(s)}(T)/\rho_b^{(s)}(0)]/dT|_{T=0}$ , since the chain band gives no contribution to the linear temperature term of  $\rho_b^{(s)}$  at low  $T$ . As a 1D pairing state has a finite energy gap under ordinary circumstances, the presence of nodes suggests that the gap function of the chain band must have 2D character, i.e. inter-chain pairing exists even though direct inter-chain hopping does not exist in the chain layer.

Because of the 1D character of the CuO chains, the wavefunction overlap between O  $2p$  and Cu  $4s$  orbitals on the CuO chain layers does not have the  $d_{x^2-y^2}$  symmetry. This changes the  $k_{\parallel}$  dependence of  $\varepsilon_{\perp k}$  and leads to a finite  $\varepsilon_{\perp}$  along  $k_x = \pm k_y$ . Besides, the CuO<sub>2</sub> planes in YBCO are dimpled with relative displacements of O in the  $c$  direction. The O displacements further reduce the crystal symmetry and introduce a noticeable hybridization between the  $\sigma$  and  $\pi$  bands. This hybridization will also make  $\varepsilon_{\perp}$  finite along the zone diagonals. Thus in YBCO,  $\varepsilon_{\perp}$  is not simply proportional to  $(\cos k_x - \cos k_y)^2$  and  $\rho_s^c$  will not follow that characteristic  $T^5$  behavior at low  $T$ .

In order to understand the low temperature behavior of  $YBa_2Cu_3O_{7-\delta}$ , let us consider a weak coupling BCS model of alternately stacking planar ‘‘CuO<sub>2</sub>’’ and chain ‘‘CuO’’ layers along the  $c$ -axis<sup>14,31,32</sup>:

$$H = H_0 + H_1, \quad (9)$$

$$H_0 = \sum_{k\sigma} (c_{1k\sigma}^\dagger \ c_{2k\sigma}^\dagger) \begin{pmatrix} \varepsilon_{1k} & \varepsilon_{\perp k} \\ \varepsilon_{\perp k} & \varepsilon_{2k} \end{pmatrix} \begin{pmatrix} c_{1k\sigma} \\ c_{2k\sigma} \end{pmatrix},$$

$$H_1 = \sum_{\alpha=1,2;k} \Delta_{\alpha k} (c_{\alpha-k\downarrow} c_{\alpha k\uparrow} + h.c.),$$

where  $c_{1k\sigma}$  and  $c_{2k\sigma}$  are electron operators in the plane and chain bands, respec-

tively. To mimic the electronic structures of YBCO-type materials, we assume the energy dispersions of the uncoupled plane and chain bands to be

$$\begin{aligned}\varepsilon_{1k} &= -2t(\cos k_x + \cos k_y) - 4t' \cos k_x \cos k_y - \mu, \\ \varepsilon_{2k} &= -2t_c \cos k_y - \mu_c,\end{aligned}$$

where  $\mu$  and  $\mu_c$  are the chemical potentials of the plane and chain bands, respectively. The coupling between the chains and planes is introduced by the nearest neighbor interlayer hopping of electrons

$$\varepsilon_{\perp k} = -2t_{\perp} \cos(k_z/2),$$

which vanishes at the zone boundary  $k_z = \pi$ .  $t_{\perp}$  is the interlayer hopping constant and is in general a function of  $k_{\parallel}$ . However, since  $t_{\perp}$  is finite in the vicinity of  $d_{x^2-y^2}$  gap nodes, we can take  $t_{\perp}$  as a  $k_{\parallel}$ -independent constant, when we discuss low temperature properties of  $H$ . For YBCO,  $t_c$  is of the same order as  $t$ , but  $t_{\perp}$  is much smaller than  $t$  or  $t_c$ .

The interlayer hopping hybridizes the plane and chain bands, and the energy dispersions of the hybridized plane and chain bands are given by

$$\tilde{\varepsilon}_{\alpha k} = \frac{\varepsilon_{1k} + \varepsilon_{2k} \pm \sqrt{(\varepsilon_{1k} - \varepsilon_{2k})^2 + 4\varepsilon_{\perp k}^2}}{2}, \quad (\alpha = 1, 2).$$

When  $\varepsilon_{\perp k} \neq 0$ , the chain band acquires dispersion in the  $a$  direction. The Fermi surface of these hybridized bands is determined by the solution of  $\varepsilon_{1k}\varepsilon_{2k} = \varepsilon_{\perp k}^2$ . In Fig. 2, we show the Fermi surface contours of  $\tilde{\varepsilon}_{1k}$  and  $\tilde{\varepsilon}_{2k}$  on the  $k_z = 0$  (solid curves) and  $k_z = \pi$  (dashed curves) planes. The area between the solid and dashed contours gives the  $z$  dispersions of  $\tilde{\varepsilon}_{1k}$  and  $\tilde{\varepsilon}_{2k}$ . The parameters used in Fig. 2 are chosen so that the Fermi surface contours of  $\tilde{\varepsilon}_{1k}$  and  $\tilde{\varepsilon}_{2k}$  resemble qualitatively those of YBCO as obtained by ARPES measurements.

In  $H_1$ ,  $\Delta_{1k}$  and  $\Delta_{2k}$  are the gap order parameters on the plane and chain layers, respectively. If pairing potentials exist independently (or nearly independently) on the planar and chain layers,  $\Delta_{1k}$  and  $\Delta_{2k}$  are then determined by self-consistent gap equations

$$\frac{1}{\Omega} \sum_k V_{k,k'}^{(\alpha)} \langle c_{\alpha k \uparrow} c_{\alpha -k \downarrow} \rangle = \Delta_{\alpha k'}, \quad (10)$$

where  $V_{k,k'}^{(\alpha)}$  ( $\alpha = 1, 2$ ) are pairing potentials.

When the plane and chain bands are uncoupled, there are two critical transition  $T$ , corresponding to the superconducting transitions of  $\text{CuO}_2$  planes and  $\text{CuO}$  chains, respectively. The quantum fluctuation of electrons in the chain band is very strong since  $\text{CuO}$  chains are quasi-one dimensional, and the transition temperature of  $\text{CuO}$  chains,  $T_c^{\text{chain}}$ , is in general very small compared with the transition temperature of  $\text{CuO}_2$  planes,  $T_c^{\text{plane}}$ . In this case,  $\rho_s^b(T)$  will rise abruptly below  $T_c^{\text{chain}}$  where the contribution from the  $\text{CuO}$  chains to  $\rho_s^b(T)$  becomes finite, as shown in Fig. 2 of Ref. 14. Switching on the interlayer coupling leads to single superconducting phase transition with  $T_c \approx T_c^{\text{plane}}$  and a smooth curve of  $\rho_s^b(T)$  in the whole temperature range. However, as the energy scale associated with  $T_c^{\text{chain}}$



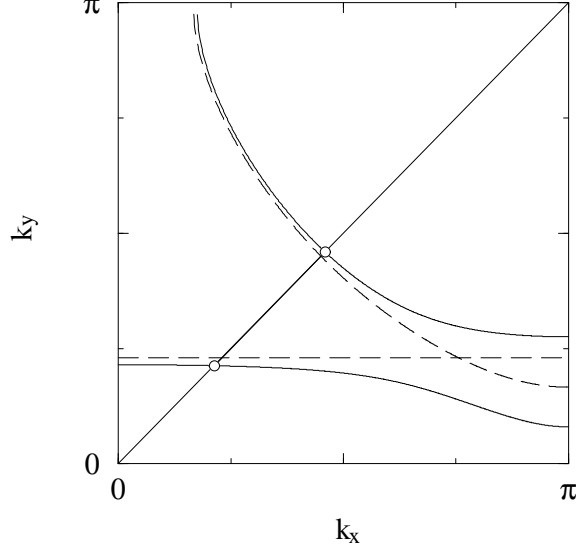


Figure 2: Fermi surfaces of  $\tilde{\varepsilon}_{1k}$  and  $\tilde{\varepsilon}_{2k}$  bands with  $k_z = 0$  (solid curves) and  $k_z = \pi/c$  (dashed curves). The circles are  $d_{x^2-y^2}$ -wave gap nodes at  $k_z = 0$  plane. The parameters used are  $t_1 = -t/4$ ,  $t_c = 1.2t$ ,  $t_z = 0.2t$ ,  $\mu = -0.6t$ , and  $\mu_c = -1.8t$ .

still exists in this system,  $\rho_s^b(T)$  will turn upwards<sup>14</sup>, i.e. have positive curvature  $\partial^2 \rho_s^b(T)/\partial T^2 > 0$ , in the vicinity of  $T_c^{\text{chain}}$ . For the same reason,  $\rho_s^c(T)$  will also turn upwards, i.e.  $\partial^2 \rho_s^c(T)/\partial T^2 > 0$ , in the vicinity of  $T_c^{\text{chain}}$ . If the CuO chain layers are not intrinsically superconducting, namely  $V_{k,k'}^{(2)} = 0$  or  $T_c^{\text{chain}} = 0$ , it can be further shown that the leading temperature dependence of  $\rho_s^b$  is

$$\rho_b \sim \sqrt{T} \quad (11)$$

at low  $T$ . This  $\sqrt{T}$  behavior of  $\rho_s^b$  has actually been found recently in double-chain  $\text{YBa}_2\text{Cu}_4\text{O}_8$  compound<sup>33</sup>. However, in  $\text{YBa}_2\text{Cu}_3\text{O}_{7-\delta}$ , this  $\sqrt{T}$  behavior or more generally the upturn curvature of  $\rho_s^{b,c}(T)$ , has not been observed in the penetration depth measurements by our group<sup>5</sup>, neither the UBC group<sup>3,4</sup>.

The absence of a positive curvature in  $\rho_s^{b,c}$  of  $\text{YBa}_2\text{Cu}_3\text{O}_{7-\delta}$  implies that  $\Delta_{2k}$  in  $\text{YBa}_2\text{Cu}_3\text{O}_{7-\delta}$  should have the same order and follow approximately the same  $T$  dependence as  $\Delta_{1k}$ . Based on this analysis, Xiang and Wheatley<sup>14,34</sup> proposed a pairing tunneling model to account for the experimental data. In this model, the gap order parameter of the planar and chain bands are strongly coupled together and  $\Delta_{\alpha k}$  are determined by

$$\frac{1}{\Omega} \sum_k V_{k,k'} \langle c_{\alpha k \uparrow} c_{\alpha -k \downarrow} \rangle = \Delta_{\bar{\alpha} k'}, \quad (12)$$

where  $\bar{\alpha} = 1$  or  $2$  if  $\alpha = 2$  or  $1$ .  $V_{k,k'}$  is the interlayer pair hopping amplitude. In Eq. (12) the gap function of the planar (chain) band is determined by the

pair correlation function of the chain (planar) band. This is the most important feature of the pair tunneling model. It will force  $\Delta_{1k}$  and  $\Delta_{2k}$  to have not only the same order of magnitude with similar temperature dependence but also the same symmetry to the leading order approximation. Thus in this model there is only one energy scale and  $\rho_s^{b,c}(T)$  will not turn upwards.

The formulae for the  $c$ -axis superfluid density in this plane-chain band model are still given by Eqs. (1) and (3), but the definitions for  $K_c$  and  $J_c$  should be changed to

$$K_c = \frac{1}{\Omega} \sum_{k\sigma} \frac{\partial^2 \varepsilon_{\perp k}}{\partial k_z^2} \langle c_{1k\sigma}^\dagger c_{2k\sigma} + h.c. \rangle, \quad (13)$$

$$J_c = \sum_{k\sigma} \frac{\partial \varepsilon_{\perp k}}{\partial k_z} (c_{1k\sigma}^\dagger c_{2k\sigma} + h.c.). \quad (14)$$

To analyse the low temperature behavior of  $\rho_s^c$ , let us first consider the case where  $\Delta_{1k} = \Delta_{2k} = \Delta_k$  and  $\Delta_k$  has  $d_{x^2-y^2}$  symmetry. In this case, the energy spectrum of superconducting quasiparticles is largely simplified, and the diamagnetic and paramagnetic terms of  $\rho_s^c$  are given by

$$K_c = -\frac{1}{\Omega} \sum_{k\alpha=1,2} \frac{\partial^2 \varepsilon_{\perp}}{\partial k_z^2} \frac{\partial E_{\alpha}}{\partial \varepsilon_{\perp}} \tanh \frac{\beta E_{\alpha}}{2}, \quad (15)$$

$$\Lambda_c = \frac{1}{\Omega} \sum_k \left[ 2 \sum_{\alpha=1,2} \left( \frac{2\varepsilon_{\perp}}{\tilde{\varepsilon}_1 - \tilde{\varepsilon}_2} \frac{\partial \varepsilon_{\perp}}{\partial k_z} \right)^2 \frac{\partial f(E_{\alpha})}{\partial E_{\alpha}} - \frac{A_{k,-}}{E_1 + E_2} + \sum_{\sigma=\pm} A_{k,\sigma} \frac{f(E_1) - \sigma f(E_2)}{E_1 - \sigma E_2} \right], \quad (16)$$

where

$$A_{k,\pm} = 2 \left( \frac{\partial \varepsilon_{\perp}}{\partial k_z} \right)^2 \frac{(\varepsilon_1 - \varepsilon_2)^2}{(\tilde{\varepsilon}_1 - \tilde{\varepsilon}_2)^2} \left( 1 \pm \frac{\tilde{\varepsilon}_1 \tilde{\varepsilon}_2 + \Delta_k^2}{E_1 E_2} \right),$$

and  $E_{\alpha k} = \sqrt{\tilde{\varepsilon}_{\alpha k}^2 + \Delta_k^2}$  is the energy dispersion of quasiparticles of the  $\alpha$  band. The gap nodes of  $E_{\alpha k}$  are located along the zone diagonal on the Fermi surface of  $\tilde{\varepsilon}_{\alpha k}$ , as shown in Fig. 2.

The diamagnetic contribution to  $\rho_s^c$ ,  $K_c$ , is proportional to the kinetic energy of the system along the  $c$ -axis. To the leading order approximation of  $t_z$ , we find that

$$K_c \approx c_1 \frac{t_z^2}{2t}, \quad (17)$$

which is temperature independent. The correction to Eq. (17) is of the order of  $\exp(-W/T)$ , with  $W$  the band width of  $\varepsilon_{1k}$  or  $\varepsilon_{2k}$ , which is negligible at low  $T$ . Here we have assumed that the energy difference between  $\tilde{\varepsilon}_{+,k}$  and  $\tilde{\varepsilon}_{-,k}$  at the same  $k$  point is on average much smaller than  $W$ .  $c_1$  is a numerical factor which depends on the detailed structures of the planar and chain bands. Numerically we found that  $c_1$  varies between 0.7 and 1.3 in a broad regime of parameters which are physically relevant. Thus approximately we can take  $c_1 = 1$ .

The first term of  $\Lambda_z$  is the intra-band contribution. Since the derivative of the Fermi function  $\partial f(E_\alpha)/\partial E_1$  is nonzero only in the vicinity of gap nodes of the  $\alpha$  band at low  $T$ , this term can be readily evaluated. For the convenience of the discussion below, we assume that the gap nodes of the  $\alpha$  band are located at  $k = Q_\alpha$  in the Brillouin zone. Around the gap nodes of the first (second) band,  $(\tilde{\varepsilon}_{1k} - \tilde{\varepsilon}_{2k})^2$  can be approximated by  $\varepsilon_{2Q_1}^2$  (or  $\varepsilon_{1Q_2}^2$ ) and taken as a constant out of the integration (or summation). To the leading order approximation in  $T$ , we find that the first term of  $\Lambda_c$  is

$$\Lambda_c^{(1)} \approx -\frac{t_\perp^4}{2} \left[ \frac{N(\varepsilon_{1,F})}{\varepsilon_{2,Q_1}^2} + \frac{N(\varepsilon_{2,F})}{\varepsilon_{1,Q_2}^2} \right] \frac{(2 \ln 2)T}{\Delta_0}, \quad (18)$$

where  $N(\varepsilon_{\alpha,F})$  is the density of states of the  $\alpha$  band at the Fermi level. Since  $\varepsilon_{\alpha Q_\alpha}$  ( $\alpha = 1, 2$ ) is of order  $t$  and  $D_{\alpha,F}$  is of order  $t^{-1}$ , we thus have  $\Lambda_c^{(1)} \sim t_\perp^4 T/t^3 \Delta_0$ , which is by a factor of  $(t_\perp/t)^2$  smaller than  $K_c$ .

The second and third terms of  $\Lambda_c$  are the inter-band contributions. The second term, which is  $T$  independent and of the same order as  $K_c$ , will cancel part of the contribution of  $K_c$  to  $\rho_s^c$ . The third term is temperature dependent. To the leading order approximation in  $T$ , we find that this term behaves as  $T^3$  at low temperature:

$$\Lambda_c^{(3)} \sim \frac{t_\perp^2 T^3}{t^3 \Delta_0}.$$

When  $T \ll t_\perp$ , this term can be ignored since it is much smaller than  $\Lambda_{(1)}$ .

We note that in this plane-chain band model the paramagnetic contribution to  $\rho_s^c$  is non-zero even at  $T = 0$ . This is a peculiar property of the model. We believe that this ‘residual’ paramagnetic current will affect the spin-lattice relaxation rate and many other properties of the system. A more comprehensive study for this model is therefore required to clarify to what extent it can be used to describe the physical properties of  $\text{YBa}_2\text{Cu}_3\text{O}_{7-\delta}$  materials.

Thus at low  $T$

$$\rho_s^c(T) \approx c'_1 \frac{t_\perp^2}{2t} \left[ 1 - c_2 \left( \frac{t_\perp}{t} \right)^2 \frac{(2 \ln 2)T}{\Delta_0} + o(T^3) \right], \quad (19)$$

where  $c'_1 < c_1$  and  $c_2$  are band-structure dependent and dimensionless constants of order 1. At zero temperature, the in-plane superfluid density  $\rho_s^{a,b}(T)$  is of order  $t$  and  $\rho_s^c(0)/\rho_s^{a,b}(0) \sim (t_\perp/t)^2$ . Since the penetration depth  $\rho_\mu \propto 1/\sqrt{\rho_s^\mu}$ , we have  $\lambda_c(0)/\lambda_{a,b}(0) \sim t/t_\perp$ . Thus from the experimental results of  $\lambda_c(0)/\lambda_{a,b}(0)$  we can estimate the value of  $t_\perp/t$ .

In the above discussion, we have assumed that  $\Delta_{1k} = \Delta_{2k}$ . In general, however,  $\Delta_{1k}$  is different from  $\Delta_{2k}$ , although they may have the same symmetry and follow approximately the same temperature dependence, such as in the pair tunneling model<sup>14</sup>. When  $\Delta_{1k} \neq \Delta_{2k}$ , an analytic treatment for the temperature dependence of  $\rho_s^c$  becomes difficult, and we therefore studied the low temperature behavior of  $\rho_s^c$  numerically. We found that in addition to the linear  $T$  contribution a  $T^2$ -term appears in  $\rho_s^c$ . In the temperature regime so far measured, this  $T^2$  term is found

to be even larger than the linear  $T$  term in a broad regime of parameters which are physically relevant. Thus at low  $T$ , we should include a  $T^2$  term in Eq. (19) and take the coefficient of this  $T^2$  term as a fitting parameter when it is used for comparison with experiment.

The linear  $T$  term of the renormalized  $c$ -axis superfluid density  $\rho_s^c(T)/\rho_s^c(0)$  is by a factor of  $(t_\perp/t)^2$  smaller than the corresponding in-plane value. This implies that this linear  $T$  term is very difficult to detect experimentally. For optimal doped YBCO,  $t_\perp/t \sim 0.2$ , it may still be possible to observe experimentally the contribution of this linear  $T$  term. For underdoped YBCO with  $t_\perp/t < 1/20$ , however, the  $T^2$  term may dominate the low  $T$  behavior of  $\rho_s^c$ .

In real YBCO materials, the system cannot be in a pure  $d_{x^2-y^2}$  pairing state because of the strong in-plane anisotropy. A more complete self-consistent solution of the gap equations should allow admixture of an s-wave component to form a d+s wave state. Admixture of a small s-component is consistent with the  $c$ -axis Josephson tunneling experiments on  $YBa_2Cu_3O_{7-\delta}$ <sup>35</sup>. The gap nodes survive for weak admixture, only the positions of the nodes shift away from the diagonals of the Brillouin zone. Thus, qualitatively, the above discussion for  $\rho_s^c$  is still valid.

#### 4 Disorder effects

Disorder effect is an important but very complicated problem in the analysis of experimental data of HTSC. For tetragonal materials, disorder is always a relevant perturbation since the  $c$ -axis hopping rate of electrons always becomes small in comparison with the impurity scattering rate when the quasiparticle momentum is sufficiently close to the nodal line. For YBCO related materials, the strong localization effect in the CuO chain layers may have a strong impact on the interlayer coupling.

In a disordered system, the quasiparticle lifetime becomes finite. This introduces a finite density of states at the Fermi level and changes the behavior of the superfluid tensor. At low  $T$ ,  $\rho_s^{ab}$  should now behave as  $T^2$  since the low energy density of states of quasiparticles varies quadratically with energy in a disordered  $d$ -wave superconductor. Along the  $c$ -axis, the singularity in  $\varepsilon_\perp$  becomes less important, and when  $T \ll \Gamma$ ,  $\rho_s^c$  can be calculated as in a disordered  $d$ -wave pairing state with a constant hopping constant, hence  $\rho_s^c$  should also behave as  $T^2$  at low  $T$ .

Another important aspect of disorder is that it may disrupt the symmetry of bonding orbitals about the copper site. The selection rule preventing hopping for momentum along  $k_x = \pm k_y$  in tetragonal HTSC is then relaxed. For example, interlayer defects on O sites may introduce a random component to  $\varepsilon_\perp$ . Near the gap nodes this fluctuating component in  $\varepsilon_\perp$  dominates the  $c$ -axis hopping, and thus electrons in the vicinity of nodes are well described by an impurity assisted hopping model<sup>16</sup>. Impurity assisted hopping gives a new conduction channel and has a direct contribution to the  $c$ -axis superfluid density  $\rho_{s,imp}^c$ .

The discussion given in this section is limited to the tetragonal high- $T_c$  materials only. Both the self-energy (or lifetime) effect and impurity assisted hopping are considered. For YBCO, a systematic analysis of the effects of disorder, considering the peculiar properties of CuO chains, is still not available.

#### 4.1 Self-energy effect

This is a commonly studied disorder effect in a  $d$ -wave superconductor. It is known that the correction from the self-energy of electrons to the diamagnetic response function  $K_\mu$  is small. Hence  $K_{ab}$  and  $K_c$  are still approximately given by the  $T$ -independent terms in Eqs. (6) and (8), respectively. However, at low  $T$ , the correction from the self-energy of quasiparticles to the paramagnetic response function  $\Lambda_\mu$  is quite significant. If we ignore the vertex correction, then  $\Lambda_\mu$  is approximately given by

$$\Lambda_\mu \approx -\frac{1}{\pi\Omega} \sum_k \left( \frac{\partial \varepsilon_k}{\partial k_\mu} \right)^2 \int d\omega f(\omega) \text{Im Tr} G^2(k, \omega), \quad (20)$$

where  $G(k, \omega)$  is the retarded electron Green's function

$$G(k, \omega) = \frac{1}{\omega - \varepsilon_k \tau_3 + \Delta_k \tau_1 + i\Gamma} \quad (21)$$

and  $\tau_{1,3}$  are Pauli matrices. The low temperature dependence of  $\Lambda_\mu$  can be readily obtained with the Sommerfeld expansion. We find that when  $T \ll \Gamma \ll \Delta_0$ ,

$$\Lambda_{ab}(T) \approx -\frac{v_F^2 N(\varepsilon_F) \Gamma}{\pi \Delta_0} \left( \ln \frac{\Delta_0}{\Gamma} + \frac{\pi^2 T^2}{6\Gamma^2} \right), \quad (22)$$

$$\Lambda_c(T) \approx -\frac{8t_\perp^2 N(\varepsilon_F) \Gamma}{3\pi \Delta_0} \left( 1 + \frac{3\pi^2 T^2}{4\Delta_0^2} \right), \quad (23)$$

where  $v_F$  is the Fermi velocity of electrons in the  $ab$  planes. Both  $\Lambda_{ab}$  and  $\Lambda_c$  are finite at  $T = 0$ . This is a direct consequence of the finite density of states at the Fermi level in a disordered  $d$ -wave superconductor.

From the results for previously obtained  $K_\mu$  and Eqs. (22) and (23), it is straightforward to calculate the normalized superfluid density. In the limit  $T \ll \Gamma$ , we have

$$\frac{\rho_s^{ab}(T)}{\rho_s^{ab}(0)} \sim 1 - \alpha_{ab} \frac{\Delta_0}{\Gamma} \left( \frac{T}{\Delta_0} \right)^2, \quad (24)$$

$$\frac{\rho_s^c(T)}{\rho_s^c(0)} \sim 1 - \alpha_c \frac{8\pi}{3} \frac{\Gamma}{\Delta_0} \left( \frac{T}{\Delta_0} \right)^2, \quad (25)$$

where  $\alpha_{ab}$  and  $\alpha_c$  are two system dependent dimensionless constants of order unity. Both  $\rho_s^{ab}(T)/\rho_s^{ab}(0)$  and  $\rho_s^c(T)/\rho_s^c(0)$  now vary quadratically with  $T$ , but the coefficients of the  $T^2$  terms are very different for the  $ab$  plane and  $c$ -axis responses. The  $T^2$  term of the  $c$ -axis response is a factor  $(\Gamma/\Delta_0)^2$  weaker than that in the  $ab$  plane due to the  $(\cos k_x - \cos k_y)^2$  factor in  $\varepsilon_{\perp k}$ . When  $\Gamma \ll T \ll \Delta_0$ , the finite lifetime effect is not important, the intrinsic behaviors of  $\rho_s^{ab}(T)$  and  $\rho_s^c(T)$ , Eqs. (6) and (8), should be recovered. The crossover temperature from the disordered  $T^2$  behavior to the intrinsic  $T$  or  $T^5$  behavior is given by the scattering rate  $\Gamma$ .

#### 4.2 Impurity assisted hopping

In Sec. 3, we showed that  $\varepsilon_{\perp k} \propto (\cos k_x - \cos k_y)^2$  for tetragonal HTSC. Effectively, we can represent this interlayer hopping integral by the following Hamiltonian:

$$H_{\perp} = \sum_{i\alpha\alpha'} t_{\perp} D_{\alpha} D_{\alpha'} c_{i+\alpha+\hat{z}}^{\dagger} c_{i+\alpha'} + h.c., \quad (26)$$

where  $D_{\alpha}$  is a function of  $\alpha$  with  $d_{x^2-y^2}$  symmetry:  $D_{\alpha} = 1/2$  or  $-1/2$  if  $\alpha = \pm\hat{x}$  or  $\pm\hat{y}$ , respectively. This Hamiltonian is clearly valid only for a clean system. If, however, impurities within or between two layers block or modify the interlayer hopping at some of the sites, then a scattering potential dependent interlayer hopping Hamiltonian

$$H_{imp}^{(1)} = \sum_{i\alpha\alpha'} W_i D_{\alpha} D_{\alpha'} c_{i+\alpha+\hat{z}}^{\dagger} c_{i+\alpha'} + h.c. \quad (27)$$

should be added to Eq. (26), where  $W_i$  is the random scattering potential.

In  $H_{imp}^{(1)}$ , we have implicitly assumed that the scattering potential preserves locally the  $d_{x^2-y^2}$  symmetry of the interlayer hopping integral. In real materials, however, this local symmetry may not always be preserved by random scatterers. The contribution from those random scatterers which do not preserve this local symmetry should also be included in the impurity assisted hopping integral. For simplicity, we assume that the interlayer hopping assisted by those scatterers has the form

$$H_{imp}^{(2)} = \sum_i V_i (c_{i+\hat{z}}^{\dagger} c_i + h.c.), \quad (28)$$

where  $V_i$  is the scattering potential. Therefore, the total impurity assisted hopping integral of electrons is  $H_{imp} = H_{imp}^{(1)} + H_{imp}^{(2)}$ .

In HTSC, the interlayer coupling is weak. Thus we can take  $H_{imp}$  as a perturbation to calculate its contribution to  $\rho_s^c$ . Up to the second order approximation in  $H_{imp}$ , we find that

$$\begin{aligned} \rho_{s,imp}^c &\sim -\frac{4}{\beta} \sum_{k,k'} \langle M_{k,k'} M_{k',k} \rangle_{imp} \int_{-\infty}^{\infty} d\omega f(\omega) \\ &\quad \text{Tr} [\text{Re}G(k, \omega) \text{Im}G(k', \omega) \\ &\quad - \text{Re}G(k, \omega) \tau_3 \text{Im}G(k', \omega) \tau_3], \end{aligned} \quad (29)$$

where  $M_{k,k'} = V_{k-k'} + W_{k-k'} \gamma_k \gamma_{k'}$  and  $\gamma_k = (\cos k_x - \cos k_y)$ . The impurity average of the assisted hopping matrix element  $\langle M_{k,k'} M_{k',k} \rangle_{imp}$  can be separated into three terms

$$\langle M_{k,k'} M_{k',k} \rangle_{imp} = V_{k-k'}^{(1)} + V_{k-k'}^{(2)} \gamma_k \gamma_{k'} + V_{k-k'}^{(3)} \gamma_k^2 \gamma_{k'}^2,$$

where  $V_k^{(1)} = \langle V_k V_{-k} \rangle_{imp}$ ,  $V_k^{(2)} = \langle V_k W_{-k} + W_k V_{-k} \rangle_{imp}$ ,  $V_k^{(3)} = \langle W_k W_{-k} \rangle_{imp}$ . The second term has the same form as Hirschfeld *et al*<sup>17</sup> assumed for the scattering potential with pair fluctuations between layers. But here this term comes purely from the single particle scattering potential.

The contribution of the first term of  $\langle M_{k,k'} M_{k',k} \rangle_{imp}$  to  $\rho_{s,imp}^c$  was first considered by Radtke *et al*<sup>16</sup>. If  $V_{k-k'}^{(1)}$  is independent on  $k-k'$  (this corresponds to a diffuse

transmission of electrons between layers), then the contribution of this term to  $\rho_s^c$  is zero. This is a special consequence of an isotropic scattering matrix element and does not hold when anisotropy due to the  $d$ -wave superconducting fluctuation is included. If, however, the scattering potential is anisotropic and long range correlated, for example if  $V_{k-k'}^{(1)}$  has the Lorentzian form<sup>16</sup>  $V_{k-k'}^{(1)} = V_1 k_F \delta k / [(\mathbf{k} - \mathbf{k}')^2 + (\delta k)^2]$ , then in the strong forward scattering limit  $\delta k / k_F \rightarrow 0$ ,  $\rho_{s,imp}^c$  behaves as  $T^2$  at low  $T$ <sup>15</sup>:

$$\rho_{s,imp}^{c,1} \approx 2\pi V_1 \Delta_0 N^2(\varepsilon_F) \left[ 1 - 8 \ln 2 \left( \frac{T}{\Delta_0} \right)^2 \right]. \quad (30)$$

For a small but finite  $\delta k$ ,  $\rho_{s,imp}^c$  behaves similarly to the  $\delta k \rightarrow 0$  case, but the overall amplitude of  $\rho_{s,imp}^c$  decreases with increasing  $\delta k$ .

The contribution of the second term of  $\langle M_{k,k'} M_{k',k} \rangle$  to  $\rho_{s,imp}^c$  has been studied recently by Hirschfeld *et al*<sup>17</sup>. If  $V_{k-k'}^{(2)} = V_2$  is dependent on  $k - k'$ , then the contribution of this term  $\rho_{s,imp}^c$  at low temperature is

$$\rho_{s,imp}^{c,2} \approx \pi V_2 N^2(\varepsilon_F) \Delta_0 \left[ 1 - \frac{12\zeta(3)}{\pi} \left( \frac{T}{\Delta_0} \right)^3 \right]. \quad (31)$$

We note that the sign of  $V_2$  is very important here. If  $V_2$  is negative,  $\rho_{s,imp}^{c,2}$  is also negative, which is obviously unphysical. Thus when  $V_2 < 0$ , the above calculation based on the second order perturbation is invalid and higher order corrections of  $H_{imp}^{(1)}$  to  $\rho_{s,imp}^{c,2}$  should be considered.

The contribution from the third term of  $\langle M_{k,k'} M_{k',k} \rangle$  to  $\rho_{s,imp}^c$  is zero if  $V_{k-k'}^{(3)}$  is a constant independent of  $k - k'$ . The reason for this is that the average of  $\gamma_k^3$  (one of the  $\gamma_k$  is from the gap function) over the Fermi surface is zero.

### 4.3 Summary

The above discussion indicates that both lifetime effects and impurity assisted hopping may give a large contribution to  $\rho_s^c$  at low  $T$ . The intrinsic  $T^5$  behavior of  $\rho_s^c$  is therefore observable only in samples which are pure and of relatively low anisotropy so that the contribution from the coherent interlayer tunneling to  $\rho_s^c$  is substantially larger than that from disorder effects. In all compounds and at sufficiently low  $T$ ,  $\rho_s^c$  should eventually behave as  $T^2$  or  $T^3$  depending on which type of disorder effects is stronger. If the contribution from the lifetime effect or the first term of  $\langle M_{k,k'} M_{k',k} \rangle_{imp}$  is larger,  $\rho_s^c$  varies as  $T^2$  at low  $T$ ; whereas if the contribution from the second term of  $\langle M_{k,k'} M_{k',k} \rangle_{imp}$  is larger,  $\rho_s^c$  varies as  $T^3$  at low  $T$ .

Disorder has opposite effects in the  $ab$  plane and along the  $c$ -axis: it weakens the  $T$ -dependence of the in-plane response and strengthens the  $T$ -dependence of the out of plane response. As will be shown later, this result agrees well with experiments. We believe it is valid also for YBCO related materials although our discussion in this section is for tetragonal HTSC only.

## 5 Experimental results

### 5.1 Technique

There are four main techniques for measuring the penetration depth  $\lambda(T)$ , namely optical conductivity, microwave surface impedance, muon spin relaxation, and low field ac magnetic susceptibility. The optical conductivity technique has been used to determine the absolute value of  $\lambda(0)$ ; measurements as a function of temperature are in principle possible but time consuming. The microwave method can be used to determine the relative change of  $\lambda(T)$  with respect to  $\lambda(0)$  accurately, but not  $\lambda(0)$  itself. Muon spin relaxation measurements can be used to determine the in-plane penetration depth at  $T = 0$ . The method we used is the ac susceptibility technique, with which we can simultaneously determine  $\lambda(0)$  directly as well as  $\lambda(T)$  both parallel and perpendicular to the CuO planes.

Two susceptometers were used in our ac susceptibility measurements. One susceptometer is home-made and is used to measure the susceptibility in the  $T$  range 1.2 - 40 K. The second susceptometer, which is commercially available, was used to obtain data in the temperature range 4.2 - 150 K. To achieve the maximum sensitivity, powder samples, with grain sizes typically of the order of a few microns, were used. To align the samples, the high- $T_c$  powders were mixed with a 5min fast curing epoxy and placed in a high static field at room temperature until the epoxy cures. The misalignment of the CuO planes of the samples is generally of the order of  $1^\circ$  for more than 95% of the grains. However, the surface of the sample can be easily contaminated when the bulk polycrystalline sample is ground into fine powder. To obtain a clean surface, we prepared the sample either by grinding the bulk ceramic in an argon atmosphere, or by heat treating the powder after grinding in air<sup>5,9,10,36,37,38</sup>

If we assume that all grains are spherical, then  $\lambda$  can be estimated from the magnetization according to the formula<sup>39</sup>

$$\frac{M}{M_0} = \frac{\int dR \left( 1 - \frac{3\lambda}{R} \coth \frac{R}{\lambda} + \frac{3\lambda^2}{R^2} \right) R^3 g(R)}{\int dR R^3 g(R)} \quad (32)$$

where  $R$  is the grain radius and  $g(R)$  is the distribution function of  $R$ <sup>40</sup>.  $M_0$  is the diamagnetic moment of a unpenetrated sample and it can be calculated from the mass of the powder.

To determine the grain size distribution function  $g(R)$ , we took scanning electron microscopy photographs for the powders and measured the dimensions of all grains along two perpendicular axes. These photographs also show that more than 80% of the grains are nearly spherical. The distribution function  $g(R)$  such determined may have a certain error. We find that the value of  $\lambda$  obtained from Eq. (32) is not sensitive to the detailed form of  $g(R)$ . For example, reducing the number of grains measured by half leads to only a 3% change in  $\lambda$  and no change in the  $T$  dependence of  $\lambda$ . Deviation from the spherical geometry tends to increase the actual surface-area to volume ratio, and effectively change the distribution function  $g(R)$ . This effect is less important when  $\lambda \sim R$  where the ratio of the penetrated to unpenetrated sample volume is similar for both spherical and non-spherical specimens. A large grain contributes a larger diamagnetic signal than a small one, thus



Table 1:  $T_c$  and zero temperature  $\lambda_{ab}(0)$  and  $\lambda_c(0)$  for several high- $T_c$  materials.

Compounds	$T_c$ (K)	$\lambda_{ab}(0)$ (Å)	$\lambda_c(0)$ (Å)	References
Ba <sub>0.6</sub> K <sub>0.4</sub> BiO <sub>3</sub>	25		3500	10
HgBa <sub>2</sub> CuO <sub>4+δ</sub>	93	1710	13600	9
HgBa <sub>2</sub> Ca <sub>2</sub> Cu <sub>3</sub> O <sub>8+δ</sub>	135	1770	61000	10,9
YBa <sub>2</sub> Cu <sub>3</sub> O <sub>7</sub>	92	1400	12600	5,36
YBa <sub>2</sub> Cu <sub>3</sub> O <sub>6.7</sub>	66	2100	45300	5
YBa <sub>2</sub> Cu <sub>3</sub> O <sub>6.57</sub>	56	2900	71700	5
YBa <sub>2</sub> (Cu <sub>1-x</sub> Zn <sub>x</sub> ) <sub>3</sub> O <sub>7</sub> (x = 0.02)	68	2600	14200	36
(x = 0.03)	55	3000	15500	36
(x = 0.05)	46	3700	16400	36

the measured susceptibility is very sensitive to the number of large grains when the majority of grains are comparable to the penetration depth in size. The uncertainty in the grain size can be reduced by sieving or sedimenting the powder before alignment.

Intergrain contacts may affect the behavior of  $\lambda$  as well. However, from the analysis of the linearity of the susceptibility in an ac field from 0.3 to 10 Gauss with frequency from 33 to 667 Hz, we find that the error resulted from this effect is less than 2%. Another possible source of error comes from the error in  $M_0$ . To determine  $M_0$  accurately, it is important to estimate accurately the mass of superconductor in the superconductor-epoxy composite. The error in  $M_0$  is mainly from the sedimentation of the grains during the alignment procedure. To reduce this error we used a fast curing epoxy and ensured that our results were reproducible between different samples cut from the same superconductor-epoxy composite. We note that none of the above errors affect the temperature dependence of  $\lambda$ . A uncertainty of 5% in the degree of grain alignment (which is higher than we usually encounter) yields at most 25% and 8% error in  $\lambda_{ab}(0)$  and  $\lambda_c(0)$ , respectively. The corresponding uncertainty in the low temperature dependence in  $\lambda_{ab}(T)/\lambda_{ab}(0)$  is at most 10% whereas it is negligible in  $\lambda_c(T)/\lambda_c(0)$ .

When the external field is parallel to the c-axis of the grains, the value of  $\lambda$  calculated from Eq. (32) is simply the in-plane penetration depth  $\lambda_{ab}$  since the diamagnetic screening current flows entirely within the ab-plane. However, when the external field is parallel to the ab-plane, the screening currents flow in both the ab plane and c axis. In this case, only an effective penetration depth,  $\lambda_{eff}$ , can be obtained from Eq. (32). An approximate solution<sup>36,39</sup>,  $\lambda_{eff} \sim 0.7\lambda_c$  in the limit  $\lambda_c \gg \lambda_{ab}$  can be used to estimate  $\lambda_c$ . The systematic error in  $\lambda_c$  obtained in such a way is less than  $\pm 2.5\%$  even when  $\lambda_c(0)/\lambda_{ab} \sim 4$ .

## 5.2 Results

We have measured the penetration depth of slightly overdoped HgBa<sub>2</sub>CuO<sub>4+δ</sub> (Hg1201), slightly underdoped HgBa<sub>2</sub>Ca<sub>2</sub>Cu<sub>3</sub>O<sub>8+δ</sub> (Hg1223), YBa<sub>2</sub>Cu<sub>3</sub>O<sub>7-δ</sub> ( $\delta = 0.0, 0.30$  and  $0.43$ ) and YBa<sub>2</sub>(Cu<sub>1-x</sub>Zn<sub>x</sub>)<sub>3</sub>O<sub>7</sub> (x=0.02, 0.03 and 0.05). A few parameters for these materials are given in Table I.  $\gamma = \lambda_c(0)/\lambda_{ab}(0)$  is an important quantity in

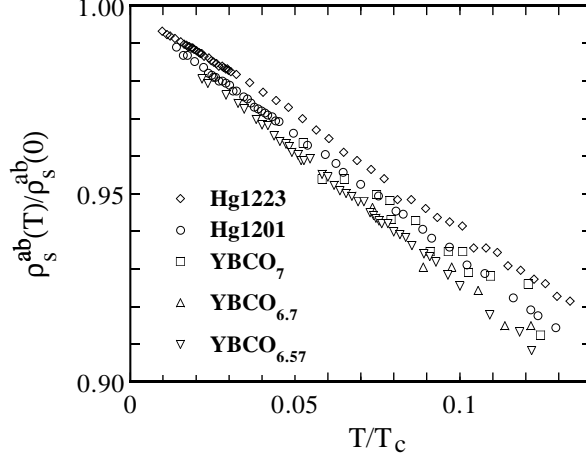


Figure 3: Normalized in-plane superfluid density  $\rho_s^{ab}(T)/\rho_s^{ab}(0)$  vs  $T/T_c$  for Hg1201, Hg1223, YBCO<sub>7</sub>, YBCO<sub>6.7</sub>, and YBCO<sub>6.57</sub> at low temperature.

characterizing the interlayer coupling. The one-layer tetragonal compound Hg1201 has the lowest anisotropy among all tetragonal HTSC,  $\gamma \sim 8$ . The three-layer tetragonal compound Hg1223 has a higher  $T_c$  (135K) as well as a higher  $\gamma$  ( $\sim 34$ ) than Hg1201. The anisotropic ratios of YBCO materials depend strongly on the doping level. With increasing oxygen deficiency,  $T_c$  of YBCO drops but  $\gamma$  increases.  $\gamma$  for YBCO<sub>7</sub>, YBCO<sub>6.7</sub>, YBCO<sub>6.57</sub> are 9, 22, and 26, respectively. Zn substitution replaces the planar Cu atoms and strongly suppresses  $T_c$ . In Zn doped YBCO, both  $\lambda_{ab}$  and  $\lambda_c$  were found to increase with Zn concentration, but  $\gamma$  drops from 9 for  $x = 0$  to 4.4 for  $x = 0.05$ .

Fig. 3 shows the reduced in-plane superfluid density  $\rho_s^{ab}(T)/\rho_s^{ab}(0)$  as a function of the reduced temperature  $T/T_c$  for the three YBCO and two Hg-related compounds at low  $T$ . The linear  $T$  dependences of  $\rho_s^{ab}$  at low  $T$  in these materials are consistent with the recent microwave measurement results of YBCO<sup>4</sup>, Bi<sub>2</sub>Sr<sub>2</sub>CaCu<sub>2</sub>O<sub>8+δ</sub><sup>7,8</sup> and Tl<sub>2</sub>Ba<sub>2</sub>CuO<sub>6+δ</sub><sup>11</sup> single crystals, indicating that the high- $T_c$  pairing has indeed  $d$  symmetry, independent on the number of CuO<sub>2</sub> planes per unit cell, carrier concentration, crystal symmetry, anisotropy and the presence of chains.

For all the compounds, both the zero temperature penetration depth and the slope of the linear  $T$  term of  $\lambda_{ab}$  are very different. For example, the coefficients of the linear  $T$  term of  $\lambda_{ab}$  are 6.5Å/K, 4.2Å/K, 4.8Å/K, 12Å/K, and 20Å/K for Hg1201, Hg1223, YBCO<sub>7</sub>, YBCO<sub>6.7</sub>, and YBCO<sub>6.57</sub>, respectively. We note, however, that the reduced superfluid density  $\rho_s^{ab}(T)/\rho_s^{ab}(0)$  as a function of  $T/T_c$  does not change much for all five samples. If we fit the data with the weak-coupling BCS result, Eq. (6), we find that  $\Delta_0$  scales approximately with  $T_c$ ,  $\Delta_0 \sim 2T_c$ , for these materials.

This approximate scaling behavior of  $\Delta_0$  with  $T_c$  is undoubtedly an important property of HTSC. However, AREPS<sup>18</sup> and tunneling<sup>41</sup> experiments have shown

that the maximum energy gap is much larger than what expected from the weak-coupling BCS theory and  $\Delta_0/T_c$  increases rapidly with decreasing doping in the underdoped regime. A possible explanation for this discrepancy is that the gap amplitude  $\Delta_0$  in the  $d$ -wave gap function  $\Delta_k = \Delta_0 \cos 2\phi$  is strongly  $\phi$ -dependent rather than simply a constant: the energy gap given by ARPES or tunneling spectroscopy measurements is the maximum gap, namely  $\Delta_{max} = \Delta_0(\phi)$  at  $\phi = 0$  or  $\pi/2$ ; whereas  $\Delta_0$  determined from low  $T$  in-plane penetration depth measurement is that around the gap nodes, namely at  $\phi = \pi/4$ .

This explanation is in fact consistent with recent ARPES measurements<sup>42</sup> which show that in the normal phase of underdoped materials, a pseudogap opens first around  $\phi = 0, \pi/2$  at high temperature and then spreads towards the  $d$ -wave gap nodes with decreasing  $T$ . Thus the effect of the pseudogap on the superconducting gap parameter is largest at  $\phi = 0$  and  $\pi/2$ , and smallest at  $\phi = \pi/4$ . Hence, although  $\Delta_0$  at  $\phi = 0, \pi/2$  does not scale with  $T_c$  in underdoped materials,  $\Delta_0$  at  $\phi = \pi/4$  does. This also explains why in the overdoped regime, where the pseudogap is very small if not completely absent, the superconducting gap  $\Delta_0$  obtained from ARPES and tunneling scales approximately with  $T_c$ .

Along the  $c$ -axis, the low  $T$  behavior of the superfluid response function is strongly sample dependent. A common feature observed in all the materials we measured is that the variation of  $\rho_s^c(T)/\rho_s^c(0)$  with  $T$  is weaker than its in-plane counterpart.

For Hg1201 (Figure 4), we find that  $\rho_s^c$  behaves as  $T^5$  at low  $T$  in agreement with theoretical prediction Eq. (8). From the fitting, we find that  $\Delta_0/T_c \sim 2.37$  which is close to the weak coupling BCS value,  $\Delta_0/T_c \sim 2.14$ , for a  $d$ -wave superconductor. In Figure 4, a comparison between the  $T^5$  and an exponential fit to the experimental data is also shown. It is clear that the exponential fit is inferior to the  $T^5$  power law fit.

The agreement between the theoretical prediction and the experimental result for the  $T^5$  behavior of  $\rho_s^c$  shows unambiguously that the gap nodes are located along the zone diagonals and the high- $T_c$  pairing has indeed the  $d_{x^2-y^2}$  symmetry. Thus the  $c$ -axis penetration depth measurement can reveal not only the existence of the gap nodes (as in the in-plane penetration depth measurement), but also the positions of the nodes on Fermi surface. This agreement also shows that the Cu  $4s$  orbital is indeed very important for understanding the interlayer dynamics and that the low energy excitations of HTSC are governed by the strongly hybridized Cu  $d_{x^2-y^2}$  and bonding O  $2p$  band (if other bands had contribution to  $\rho_s^c$ ,  $\rho_s^c$  would deviate noticeably from  $T^5$  at low  $T$  since the effective  $c$ -axis hopping integrals for these bands do not have the property  $\varepsilon_\perp \propto (\cos k_x - \cos k_y)^2$ ).

The  $T^5$  behavior of  $\rho_s^c$  for tetragonal HTSC is very small at low  $T$ . This behavior can be observed in samples which are pure and of low anisotropy so that the coherent inter-layer hopping of electrons is the main contribution to  $\rho_s^c$ . In highly anisotropic materials, however, the coherent tunneling component of the supercurrent along the  $c$ -axis is significantly reduced and the contribution from incoherent tunneling induced by disorder scattering may dominate the low  $T$  behavior of  $\rho_s^c$ . Thus the low  $T$  behavior of  $\rho_s^c$  for a highly anisotropic HTSC is expected to be different than for HTSCs with lower anisotropy.

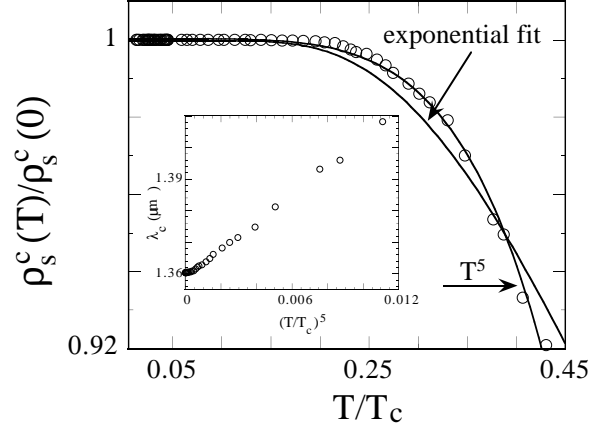


Figure 4:  $\rho_s^c(T)/\rho_s^c(0)$  vs  $T/T_c$  for Hg1201 at low  $T$ . A comparison between a  $T^5$  power law and an exponential fit to the experimental data is given. The inset shows the experimental data of the  $c$ -axis penetration depth  $\lambda_c$  as a function of  $(T/T_c)^5$ .

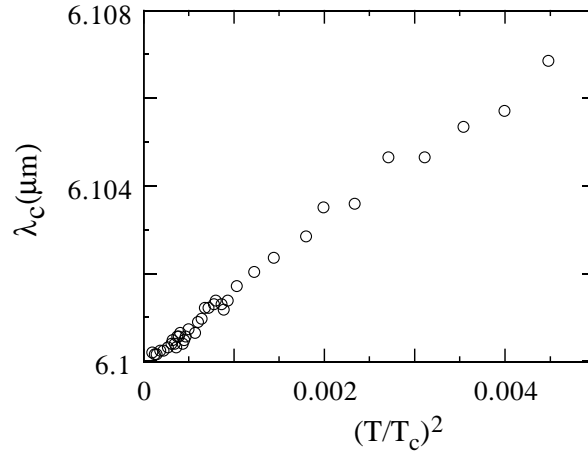


Figure 5: Low  $T$   $\lambda_c$  vs  $(T/T_c)^2$  for Hg1223.

For Hg1223, the  $c$ -axis penetration depth  $\lambda_c(T)$  varies quadratically with  $T$  at low  $T$  (Fig. 5). This  $T^2$  term probably arises from disorder effects which, as discussed in Sec. 4, can give rise to a  $T^2$  term in  $\rho_s^c(T)$  without significantly affecting the linear  $T$  term in  $\lambda_{ab}(T)$ .

Figures 6(a) and 6(b) shows the normalized  $c$ -axis superfluid densities as functions of  $T/T_c$  for YBCO<sub>7</sub> and  $(T/T_c)^2$  for YBCO<sub>6.7</sub> and YBCO<sub>6.57</sub>, respectively.  $\lambda_c$  for YBCO<sub>7</sub> ( $\gamma = 9$ ) exhibits a linear  $T$  dependence at low  $T$  but the relative change is about a factor of two smaller than in  $\lambda_{ab}(T) / \lambda_{ab}(0)$ . As discussed earlier this probably arises from the effects of hopping between planar and chain bands present in YBCO (see Eq. (19)). By removing oxygen from YBCO<sub>7</sub> one can reduce the effects of the chains.  $\lambda_c(T)$  of YBCO<sub>6.7</sub> ( $\gamma \sim 22$ ) and YBCO<sub>6.57</sub> ( $\gamma \sim 25$ ) vary as  $T^2$ , like Hg-1223 which has similar anisotropy.

Figure 7 shows the normalized in-plane (a) and  $c$ -axis (b) superfluid density as a function of  $T/T_c$  for YBa<sub>2</sub>(Cu<sub>1-x</sub>Zn<sub>x</sub>)<sub>3</sub>O<sub>7</sub> with  $x=0.02, 0.03$  and  $0.05$ . As shown in Table I,  $\lambda_{ab}(0)$  increases very quickly with Zn doping. This fast increase of  $\lambda_{ab}(0)$  is consistent with an increase in the residual density of states as revealed by the measurement of low temperature specific heat<sup>43</sup>. The increase of  $\lambda_c(0)$  with Zn concentration is relatively slower, which may be due to an enhanced  $c$ -axis coupling caused by Zn doping. The low  $T$  dependences of both  $\lambda_{ab}$  and  $\lambda_c$  change from  $T$  to  $T^2$  with Zn doping due to impurity scattering. Another interesting property of Zn doped YBCO is that with increasing doping both  $\lambda_{ab}(0) / \lambda_{ab}(T)$  and  $\lambda_c(0) / \lambda_c(T)$  gradually approach each other, and for  $x = 0.05$  they have almost the same  $T$  behavior (Fig. 8).

## 6 Summary

In summary, the low  $T$  behavior of the superfluid tensor has been systematically investigated. We found that the low  $T$  slope of  $\rho_s^{ab}(0)/\rho_s^{ab}(T)$  scales approximately with  $T_c$ , irrespective of their doping level, anisotropy and chemical structures. If we assume that the weak coupling BCS theory is applicable in the low  $T$  regime of HTSC, this result implies that the gap amplitude  $\Delta_0$  scales approximately with  $T_c$  for all high- $T_c$  materials.

For tetragonal HTSC, we gave a simple symmetry argument which shows that the  $c$ -axis hopping matrix element  $\varepsilon_\perp(k_\parallel) \propto (\cos k_x - \cos k_y)^2$  and that for low anisotropic Hg1201  $\rho_s^c$  behaves as  $T^5$  at low  $T$ . For more anisotropic materials, such as Hg1223,  $\rho_s^c(T)$  behaves as  $T^2$  at low  $T$  due to disorder effects.

The planar anisotropy of electromagnetic response of clean YBCO-type structures gives a useful probe of the microscopic state of cuprate superconductors. If the superfluid density on the CuO chains is induced purely by the proximity effect,  $\lambda_b$  is shown to behave as  $\sqrt{T}$  at low  $T$ . If on the other hand, the pair tunneling (or Josephson tunneling) process between CuO chains and CuO planes is important,  $\lambda_b$  varies linearly with  $T$  at low  $T$ . The experimental data of YBa<sub>2</sub>Cu<sub>3</sub>O<sub>7- $\delta$</sub>  agree with the pair tunneling picture, but the low  $T$  behavior of YBa<sub>2</sub>Cu<sub>4</sub>O<sub>8</sub> seem to be consistent with the result of the proximity model. Why the low  $T$   $\lambda_b$  of YBa<sub>2</sub>Cu<sub>3</sub>O<sub>7- $\delta$</sub>  and that of YBa<sub>2</sub>Cu<sub>4</sub>O<sub>8</sub> behave so differently requires further theoretical investigation.

The effect of disorder on the low  $T$  behavior of the superfluid tensor is more

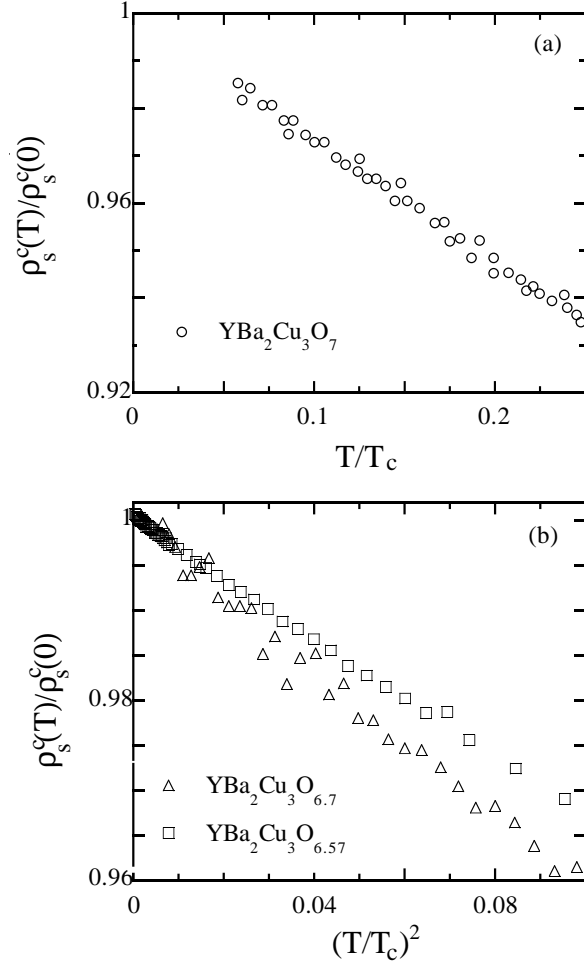


Figure 6:  $\rho_s^c(T)/\rho_s^c(0)$  as a function of (a)  $T/T_c$  for  $\text{YBCO}_7$  and (b)  $(T/T_c)^2$  for  $\text{YBCO}_{6.7}$  and  $\text{YBCO}_{6.57}$  at low  $T$ .

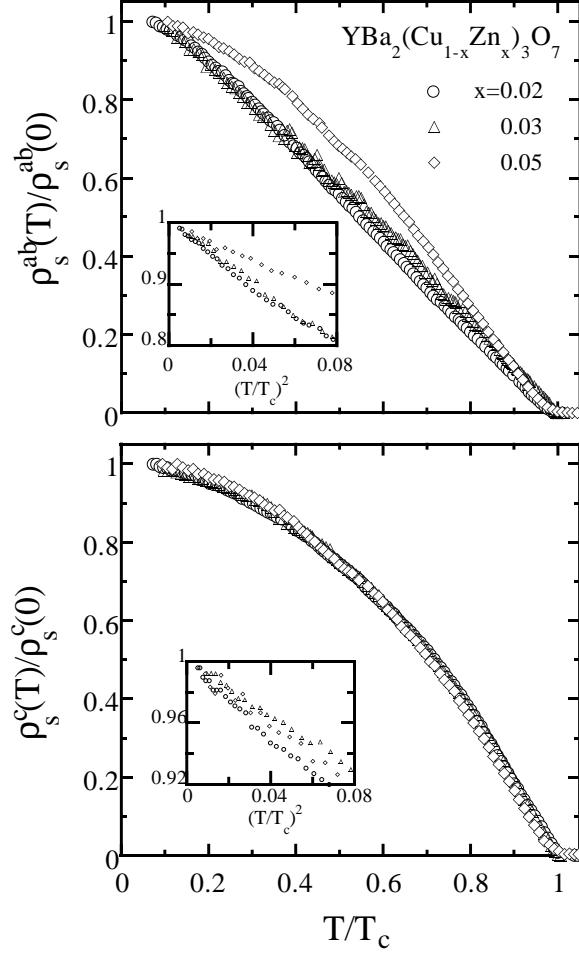


Figure 7: Normalized in-plane (a) and  $c$ -axis (b) superfluid density vs  $T/T_c$  for  $\text{YBa}_2(\text{Cu}_{1-x}\text{Zn}_x)_3\text{O}_7$  with  $x=0.02, 0.03$  and  $0.05$ . Insets show the corresponding reduced superfluid tensor as a function of  $(T/T_c)^2$  at low  $T$ .

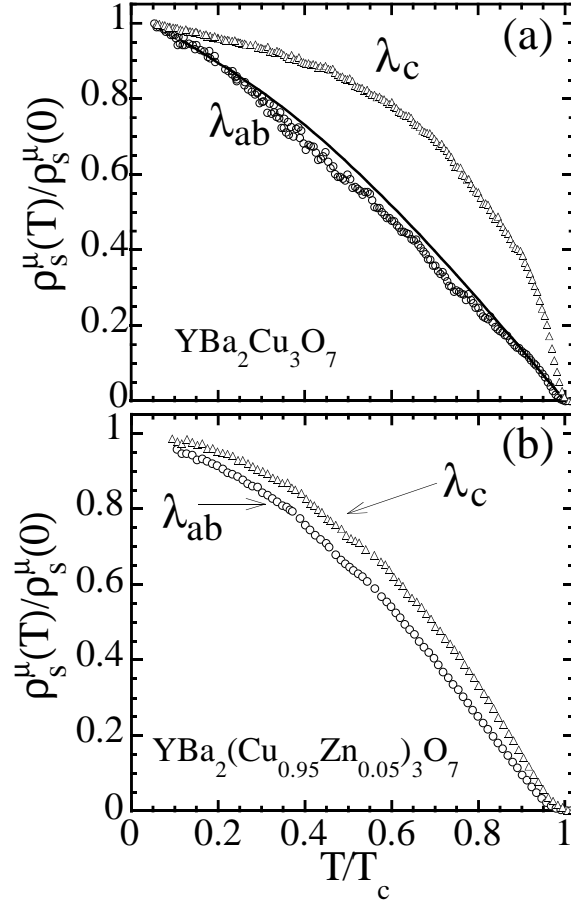


Figure 8: Comparison between the reduced in-plane and out-of-plane superfluid density as a function of  $T/T_c$  for (a)  $\text{YBa}_2\text{Cu}_3\text{O}_7$  and (b)  $\text{YBa}_2(\text{Cu}_{0.95}\text{Zn}_{0.05})_3\text{O}_7$ . The solid line in (a) is the weak-coupling BCS result for a  $d$ -wave superconductor.



apparent in heavily underdoped or Zn doped YBCO. In YBCO<sub>6.57</sub> and YBCO<sub>6.7</sub>,  $\rho_s^{ab}$  and  $\rho_s^c$  vary linearly and quadratically with  $T$  at low  $T$ , respectively. For Zn-doped YBCO, both  $\rho_s^{ab}$  and  $\rho_s^c$  behave as  $T^2$  at low  $T$ .

## References

1. See, for example, J F Annett, N Goldenfeld, and A Leggett, in Physical Properties of High Temperature Superconductors V edited by D M Ginsberg (World Scientific, Singapore, 1996).
2. W N Hardy, D A Bonn, D C Morgan, R Liang, and K Zhang, Phys. Rev. Lett. **70**, 3999 (1993).
3. K Zhang, D A Bonn, S Kamal, R Liang, D J Baar, W N Hardy, D Basov, and T Timusk, Phys. Rev. Lett. **73**, 2484 (1994).
4. D A Bonn, S Kamal, K Zhang, R Liang, and W N Hardy, J. Phys. Chem. Solids **56**, 1941 (1995).
5. C Panagopoulos, J R Cooper, T Xiang, G B Peacock, I Gameson, P P Edwards, W Schmidbauer, and J W Hodby, Physica C **282-287**, 145 (1997).
6. C Panagopoulos, J R Cooper, and T Xiang, Phys. Rev. B in press.
7. T Jacobs, S Sridhar, Q Li, G D Gu, and N Koshizuka, Phys. Rev. Lett. **75**, 4516 (1995).
8. S Lee, D C Morgan, R J Ormeno, D M Broun, R A Doyle, J R Waldram, and K Kadowaki, Phys. Rev. Lett. **77**, 735 (1996).
9. C Panagopoulos, J R Cooper, T Xiang, G B Peacock, I Gameson, and P P Edwards, Phys. Rev. Lett. **79**, 2320 (1997).
10. C Panagopoulos, J R Cooper, G B Peacock, I Gameson, P P Edwards, W Schmidbauer and J W Hodby, Phys. Rev. B **53**, R2999 (1996).
11. D M Broun, D C Morgan, R J Ormeno, S F Lee, A W Tyler, A P Mackenzie, J R Waldram, Physica C **282**, 1467 (1997); Phys. Rev. **56**, 11443 (1997).
12. C Panagopoulos *et al.*, unpublished.
13. T Shibauchi, H Kitano, K Uchinokura, A Maeda, T Kimura, and K Kishio, Phys. Rev. Lett. **72**, 2263 (1994).
14. T Xiang and J M Wheatley, Phys. Rev. Lett. **76**, 134 (1996).
15. T Xiang and J M Wheatley, Phys. Rev. Lett. **77**, 4632 (1996).
16. R J Radtke, V N Kostur, and K Levin, Phys. Rev. B **53**, 522 (1996).
17. P J Hirschfeld, S M Quinlan, D J Scalapino, Phys. Rev. B **55**, 12742 (1997).
18. See, for example, M Randeria and J Campuzano, cond-mat/9709107 and references therein.
19. D A Bonn, P Dosanjh, R Liang, and W N Hardy, Phys. Rev. Lett. **68**, 2390 (1992).
20. K Krishana, J M Harris and N P Ong, Phys. Rev. Lett. **75**, 3529 (1995).
21. D J Scalapino, S R White, and S C Zhang, Phys. Rev. Lett. **68**, 2830 (1992).
22. F C Zhang and T M Rice, Phys. Rev. B **37**, 3759 (1988).
23. O. K. Andersen, A. I. Liechtenstein, O. Jepsen, and F. Paulsen, J. Phys. Chem. Solids, **56**, 1573 (1995).
24. T Xiang, C Panagopoulos, and J R Cooper, in "Proceedings of the IX International Conference on Recent Progress in Many Body Theories" (1997).

25. See, for example, D L Novikov and A J Freeman, *Physica C* **216**, 273 (1993).
26. D N Basov, R Liang, D A Bonn, W N Hardy, B Dabrowski, M Quijada, D B Tanner, J P Rice, D M Ginsberg, and T Timusk, *Phys. Rev. Lett.* **74**, 598 (1995).
27. J L Tallon, C Bernhard, U Binniger, A Hofer, G V M Williams, E J Ansaldo, J I Budnick, and Ch Niedermayer, *Phys. Rev. Lett.* **74**, 1008 (1995).
28. T. A. Friedmann, M. W. Rabin, J. Giapintzakis, J. P. Rice, and D. M. Ginsberg, *Phys. Rev. B* **42** 6217 (1990).
29. T. Imai, T. Shimizu, H. Yasuoka, Y. Ueda, and K. Kosuge, *J. Phys. Soc. Jpn.* **57**, 2280 (1988).
30. M Takigawa, P C Hammel, R H Heffner, and Z. Fisk, *Phys. Rev. B* **39**, 7371 (1989).
31. R A Klemm and S H Liu, *Phys. Rev. Lett.* **74**, 2343 (1995).
32. W A Atkinson and J P Carbotte, *Phys. Rev. B* **51** 16371 (1995); **55**, 14592 (1997).
33. C Panagopoulos, J L Tallon, and T Xiang, unpublished.
34. J M Wheatley, T C Hsu, P W Anderson, *Phys. Rev. B* **37**, 5897 (1988); S Chakravarty, A Sudbo, P W Anderson, and S Strong, *Science* **261**, 337 (1993).
35. A G Sun, D A Gajewski, M B Maple, and R C Dynes, *Phys. Rev. Lett.* **72**, 2267 (1994).
36. C Panagopoulos, J R Cooper, N Athanassopoulou, and J Chrosch, *Phys. Rev. B* **54**, R12721 (1996).
37. C Panagopoulos, W Zhou, N Athanassopoulou, J R Cooper, *Physica C* **269**, 157 (1996).
38. J Chrosch, C Panagopoulos, N Athanassopoulou, J R Cooper, E K H Salje, *Physica C* **265**, 233 (1996).
39. A Porch, J R Cooper, D N Zheng, J R Waldram, A M Campbell, P A Freeman, *Physica C* **214**, 350 (1993).
40. J R Cooper, C T Chu, L W Zhou, B Dunn, G Gruner, *Phys. Rev. B* **37**, 638 (1988).
41. C Renner, B Revaz, J Y Genoud, K Kadowaki, and O Fischer, *Phys. Rev. Lett.* **80**, 149 (1998).
42. M R Norman, H Ding, M Randeria, J C Campuzano, T Yokoya, T Takeuchi, T Takahashi, T Mochiku, K Kadowaki, P Guptasarma, D G Hinks, *Nature* **392**, 157 (1998).
43. J W Loram, K A Mirza, and P A Freeman, *Physica C* **171**, 243 (1990).